

Design of Linear Combination of Weighted Medians

Kang-Sun Choi, *Student Member, IEEE*, Aldo W. Morales, *Senior Member, IEEE*, and
Sung-Jea Ko, *Senior Member, IEEE*

Abstract—This paper introduces a novel nonlinear filtering structure: the linear combination of weighted medians (LCWM). The proposed filtering scheme is modeled on the structure and design procedure of the linear-phase FIR highpass (HP) filter in that the linear-phase FIR HP filter can be obtained by changing the sign of filter coefficients of the FIR lowpass (LP) filter in the odd positions. The HP filter can be represented as the difference between two LP subfilters that have all positive coefficients. This representation of the FIR HP filter is analogous to the difference of estimates (DoE) such as the difference of medians (DoM). The DoM is essentially a nonlinear HP filter that is commonly used in edge detection. Based on this observation, we introduce a class of LCWM filters whose output is given by a linear combination of weighted medians of the input sequence. We propose a method of designing the 1-D and 2-D LCWM filters satisfying required frequency specifications. The proposed method adopts a transformation from the FIR filter to the LCWM filter. We show that the proposed LCWM filter can offer various frequency filtering characteristics including “LP,” “bandpass (BP),” and “HP” responses.

Index Terms—Image enhancement, median filters, nonlinear estimation, nonlinear filters.

I. INTRODUCTION

THE WEIGHTED median (WM) filter has been recognized as a useful smoother in signal and image processing since it preserves edges in images and is effective in suppressing impulsive noise [1]. The connection between WM filters and positive Boolean functions (PBFs) has been established using threshold decomposition [2], [3]. Some statistical and deterministic properties of WM filters have been derived using the PBF representation [2], [4], [5]. Mallows [6] derived the relationship between linear and nonlinear filters using the sample selection probability (SSP). It is further proven in [6] that the SSPs equal the impulse response coefficients of a finite impulse response (FIR) filter whose output spectrum is closest, of all linear filters, to that of the order statistic filter for independent identically distributed (i.i.d.) Gaussian inputs. Using Mallows’ approach, the WM filter can be analyzed from a spectral point of view.

The WM filter, however, does not offer much flexibility in a number of signal and image processing applications since it

is inherently a smoother with LP filtering characteristics. Recently, to solve this problem, Arce [7] proposed the general weighted median (GWM) filter admitting positive and negative weights. In the GWM filter framework, the negative sign of the weight is uncoupled from the weight magnitude value and is merged with the input sample, and thus, the weights are always positive. It is shown in [7] that this filter can exhibit HP and BP frequency characteristics. This framework has been extended to stack filters by mirrored threshold decomposition [8] and recursive WM filters [9]. In practice, it is desirable to design the weights of a filter in some optimal fashion. Some adaptive algorithms have been developed for optimizing nonlinear filters under the mean absolute error (MAE) criterion [7], [9], [10].

In this paper, we propose a class of linear combination of weighted median (LCWM) filters that can offer various frequency characteristics including LP, BP, and HP responses. The proposed scheme is modeled on the structure and design procedure of the linear-phase FIR HP filter. The FIR HP filter can be easily obtained by changing the sign of filter coefficients of the FIR LP filter in the odd positions. Thus, the HP filter can be represented as the difference between two LP subfilters that have all positive coefficients. This difference is analogous to the difference of estimates (DoE) such as the difference of medians (DoM) [11]–[15]. The DoM is essentially a robust high-frequency estimator that is commonly used in edge detection. Based on this observation, we define a new nonlinear filter whose output is given by a linear combination of weighted medians of the input sequence. We refer to this filter class as the LCWM filter [16]. In this paper, we introduce a filter design procedure for the LCWM filter using a linear-to-nonlinear mapping method.

The organization of the paper is as follows. In Section II, we review the analogy between WM filters and FIR filters. In Section III, the LCWM filter is introduced, and its frequency selectivity is demonstrated by some examples. Design methods for one-dimensional (1-D) and two-dimensional (2-D) LCWM filters are derived in Section IV. Experimental results are given in Section V. Finally, conclusions are given in Section VI.

II. ANALOGY BETWEEN WEIGHTED MEDIAN FILTERS AND FIR FILTERS

A. Estimation Theory [7]

The sample mean and the sample median are the maximum likelihood (ML) estimators of location when the input samples are i.i.d. with Gaussian and Laplacian distributions, respectively. If X_i , $i = 1, 2, \dots, N$ are N independent Gaussian and

Manuscript received May 2, 2000; revised May 21, 2001. The associate editor coordinating the review of this paper and approving it for publication was Dr. Gonzalo R. Arce.

K.-S. Choi and S.-J. Ko are with the Department of Electronics Engineering, Korea University, Seoul, Korea (e-mail: kschoi@dali.korea.ac.kr; sjko@dali.korea.ac.kr).

A. W. Morales is with Pennsylvania State University, University Park, PA 16802 USA (e-mail: awm2@psu.edu).

Publisher Item Identifier S 1053-587X(01)07049-0.

Laplacian distributed samples with unknown mean y , the likelihood functions for estimating y , respectively, are given by

$$\prod_{i=1}^N f_G(x_i; y) = \prod_{i=1}^N \left(\frac{1}{2\pi\sigma_i^2} \right)^{N/2} \exp \left(- \sum_{i=1}^N \left(\frac{X_i - y}{2\sigma_i^2} \right)^2 \right) \quad (1)$$

$$\prod_{i=1}^N f_L(x_i; y) = \prod_{i=1}^N \left(\frac{1}{2\sigma_i^2} \right)^{N/2} \exp \left(- \sum_{i=1}^N \left(\frac{\sqrt{2}}{\sigma_i^2} |X_i - y| \right) \right) \quad (2)$$

where σ_i^2 is the variance of X_i . An ML estimate of y is obtained by finding a value that maximizes the likelihood function. The estimated value \hat{y} maximizing (1) is the normalized sample mean given by

$$\hat{y} = \frac{1}{\sum_{i=1}^N 1/\sigma_i^2} \sum_{i=1}^N \frac{1}{\sigma_i^2} X_i = \sum_{i=1}^N W_i X_i. \quad (3)$$

Likewise, under the Laplacian model, the maximum likelihood estimate of location minimizes the sum of weighted absolute deviations

$$\sum_{i=1}^N \frac{1}{\sigma_i^2} |X_i - y|. \quad (4)$$

The value \hat{y} minimizing the above sum is the output of the WM filter given by

$$\hat{y} = MED[W_1 \diamond X_1, W_N \diamond X_N, \dots, W_N \diamond X_N] \quad (5)$$

where $W_i = 1/\sigma_i^2$, and \diamond is the replication operator defined as

$$W_i \diamond A = \overbrace{A, A, \dots, A}^{W_i \text{ times}}.$$

Note that the weights in (5) are of non-negative values due to their inverse relationship to the variances of the respective observation samples. From an estimation point of view, the weighted sample mean and the weighted sample median estimation scheme in (3) and (5) have analogous roots.

B. Estimated Frequency Response of the WM Smoother

Mallows' approach gives a simple analytical tool for analyzing nonlinear filters using the SSP defined as the probability that the output Y equals the i th sample X_i . With this approach, the spectral behavior of the order-statistic filter can be reasonably represented by that of an equivalent FIR filter for i.i.d. Gaussian inputs.

To illustrate that FIR and median filters exhibit similar frequency characteristics, an example is presented in Fig. 1. Fig. 1(a) illustrates the frequency responses of the FIR filters (FIR5 and FIR7) with coefficients $[1/5, 1/5, 1/5, 1/5, 1/5]$

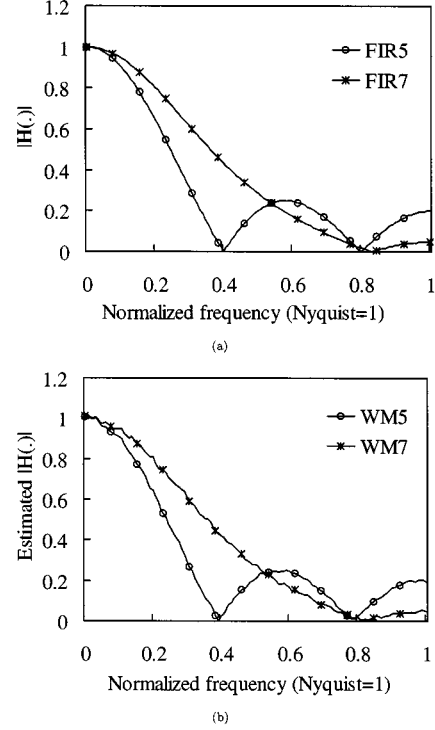


Fig. 1. Estimated frequency responses. (a) Frequency responses of FIR filters (FIR5 and FIR7). (b) Estimated frequency responses of WM smoothers (WM5 and WM7).

and $[1/70, 1/21, 78/315, 8/21, 78/315, 1/21, 1/70]$. Fig. 1(b) shows the estimated frequency responses of the WM smoothers (WM5 and WM7) with weights $[1, 1, 1, 1, 1]$ and $[1, 2, 5, 7, 5, 2, 1]$ whose SSPs correspond to the coefficients of the above FIR filters. The ratio of the Fourier transform of the output to the Fourier transform of the input was utilized to estimate the frequency response of the WM smoothers. The simulations for this paper used ten input sequences with 100 000 white Gaussian samples. Comparison of Fig. 1(a) and (b) shows that the frequency responses of the FIR and WM filters are very similar and clearly exhibit LP filtering characteristics.

III. LCWM FILTERS

In this section, we first briefly review the FIR HP filter and then propose the LCWM filter.

A. FIR HP Filter

An N -tap FIR filter is given by

$$y(n) = \sum_{k=0}^{N-1} h(k)x(n-k) \quad (6)$$

or equivalently

$$y(n) = \mathbf{h}\mathbf{x}^T \quad (7)$$

where $\mathbf{h} = [h(0) \ h(1) \ \dots \ h(N-1)]$ represents the filter coefficient vector, and $\mathbf{x} = [x(n) \ x(n-1) \ \dots \ x(n-N+1)]$ is the input vector.

For the linear-phase LP filter, the $h(k)$ s are symmetric with respect to the midpoint. Changing the sign of coefficients in

the odd positions after reversing the filter window in the time domain results in the HP filter given by

$$\begin{aligned} y_H(n) &= \sum_{k=0}^{N-1} (-1)^k h_L(N-k-1)x(n-k) \\ &= \sum_{k=0}^{N-1} h_H(k)x(n-k) \end{aligned} \quad (8)$$

where

$$h_H(k) = \begin{cases} h_L(N-k-1), & \text{if } k \text{ is even} \\ -h_L(N-k-1), & \text{otherwise.} \end{cases}$$

The HP filter in (8) can be divided into two subfilters as follows:

$$\begin{aligned} y_H(n) &= \sum_{k=0}^{N-1} h_H(k)x(n-k) \\ &= \sum_{k=0}^{N-1} b_1(k)x(n-k) - \sum_{k=0}^{N-1} b_2(k)x(n-k) \\ &= y_1(n) - y_2(n) \end{aligned} \quad (9)$$

where N is even, and $b_1(k)$ and $b_2(k)$ are given by

$$\begin{aligned} b_1(k) &= \begin{cases} h_H(k), & \text{if } h_H(k) \geq 0 \\ 0, & \text{otherwise} \end{cases} \\ b_2(k) &= \begin{cases} |h_H(k)|, & \text{if } h_H(k) < 0 \\ 0, & \text{otherwise.} \end{cases} \end{aligned} \quad (10)$$

Note that the two subfilters $y_1(n)$ and $y_2(n)$ have only non-negative coefficients $b_1(k)$ s and $b_2(k)$ s. Normalizing these coefficients gives

$$y(n) = \alpha_1 y_1^N(n) + \alpha_2 y_2^N(n) \quad (11)$$

where

$$y_1^N(n) = \frac{\sum_{k=0}^{N-1} b_1(k)x(n-k)}{\sum_{k=0}^{N-1} b_1(k)}, \quad y_2^N(n) = \frac{\sum_{k=0}^{N-1} b_2(k)x(n-k)}{\sum_{k=0}^{N-1} b_2(k)}$$

$$\alpha_1 = \sum_{k=0}^{N-1} b_1(k), \text{ and } \alpha_2 = \sum_{k=0}^{N-1} b_2(k).$$

B. LCWM Filters

Using Mallows' approach, we obtain a nonlinear filter consisting of WM subfilters that are the nonlinear counterparts of the FIR subfilters $y_1^N(n)$ and $y_2^N(n)$ in (11). Thus, the nonlinear counterpart of the linear filter in (11) is given by

$$\tilde{y}(n) = \alpha_1 y_1^{\text{WM}}(n) + \alpha_2 y_2^{\text{WM}}(n) \quad (12)$$

where $y_1^{\text{WM}}(n)$ and $y_2^{\text{WM}}(n)$ are the WM smoothers.

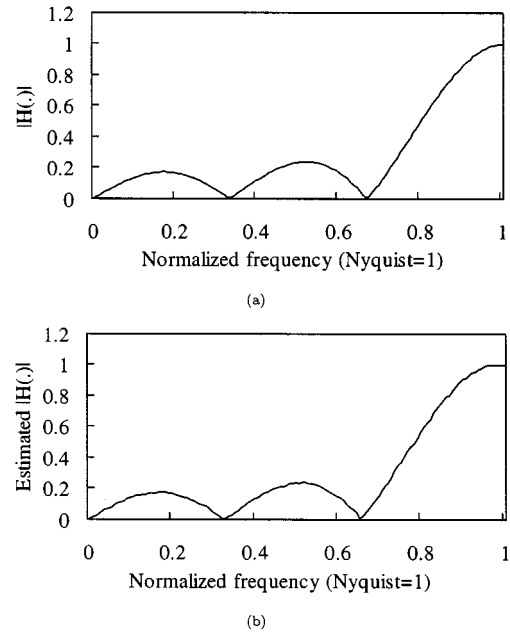


Fig. 2. (Estimated) frequency response. (a) Frequency response of FIR HP filter with coefficients $[1/6, -1/6, 1/6, -1/6, 1/6, -1/6]$. (b) Estimated frequency response of $1/2 [1 \ 0 \ 1 \ 0 \ 1 \ 0] - 1/2 [0 \ 1 \ 0 \ 1 \ 0 \ 1]$.

In a similar fashion as the vector notation of (7), let \mathbf{w} denote the weight vector of the WM smoother. Then, the WM smoother is defined by

$$\langle \mathbf{w} \rangle \triangleq \text{MED}[\mathbf{w} \diamond \mathbf{x}] \quad (13)$$

where $\mathbf{w} \diamond \mathbf{x}$ is $[w_1 \diamond x(n), w_2 \diamond x(n-1), \dots, w_N \diamond x(n-N+1)]$.

For example, the WM smoother $\langle [1 \ 0 \ 0 \ 2 \ 3 \ 0 \ 2 \ 1] \rangle$ is represented by

$$\begin{aligned} y(n) &= \text{MED}[x(n), 2 \diamond x(n-3), 3 \diamond x(n-4) \\ &\quad 2 \diamond x(n-6), x(n-7)]. \end{aligned}$$

Using vector notation, (12) can be rewritten as

$$\tilde{y}(n) = \alpha_1 \langle \mathbf{w}_1 \rangle + \alpha_2 \langle \mathbf{w}_2 \rangle. \quad (14)$$

For example, consider a linear FIR HP filter with coefficients $[1/6, -1/6, 1/6, -1/6, 1/6, -1/6]$. The above procedure gives its nonlinear counterpart $\tilde{y} = 1/2 \langle [1 \ 0 \ 1 \ 0 \ 1 \ 0] \rangle - 1/2 \langle [0 \ 1 \ 0 \ 1 \ 0 \ 1] \rangle$. Fig. 2 shows the frequency response of the linear filter and the estimated frequency response of the nonlinear counterpart. It is seen that these two filters produce similar results.

It is interesting to point out that the DoM is a special case of (14). For example, the DoM with window size 5 is given by

$$\begin{aligned} y(n) &= \text{MED}[x(n), x(n-1), x(n-2)] \\ &\quad - \text{MED}[x(n-2), x(n-3), x(n-4)]. \end{aligned}$$

In this case, $\mathbf{w}_1 = [1 \ 1 \ 1 \ 0 \ 0]$, $\mathbf{w}_2 = [0 \ 0 \ 1 \ 1 \ 1]$, $\alpha_1 = 1$, and $\alpha_2 = -1$.

The fact that an FIR filter is divided into two subfilters by the sign of coefficients would suggest that the resulting nonlinear filter has two WM subfilters with two nonoverlapping subwindows. However, since distinct WM smoothers, which are dis-

tinguished by their SSPs, are countable, this division does not always produce WM smoothers with SSPs that are identical to the divided FIR subfilter coefficients. Therefore, we consider the division of a general FIR filter into several FIR subfilters with overlapping or nonoverlapping subwindows. The only constraint is that the WM smoother corresponding to each FIR subfilter must exist. Then, we generalize (11) as

$$y(n) = \sum_{i=1}^K \alpha_i \cdot y_i(n) \quad (15a)$$

$$= \sum_{i=1}^K \alpha_i \sum_{j=0}^{N-1} b_i(j)x(n-j), \quad \alpha_i \in \mathbb{R} \quad (15b)$$

where K is the number of subfilters, and $b_i(j)$ is the $(j+1)$ th coefficient of the i th subfilter. Define the coefficient vector \mathbf{b}_i of the i th subfilter and the coefficient matrix \mathbf{B} of subfilters as follows:

$$\mathbf{b}_i = [b_i(0) \ b_i(1) \ \dots \ b_i(N-1)] \quad (16a)$$

$$\mathbf{B} = \begin{bmatrix} \mathbf{b}_1 \\ \vdots \\ \mathbf{b}_K \end{bmatrix}. \quad (16b)$$

Then, the matrix representation of (15b) is given by

$$y(n) = \boldsymbol{\alpha} \mathbf{B} \mathbf{x}^T \quad (17)$$

where $\boldsymbol{\alpha} = [\alpha_1 \ \dots \ \alpha_K]$ is referred to as the weighting factor vector. Thus, from (7) and (17), the weight factor vector $\boldsymbol{\alpha}$ is determined by

$$\boldsymbol{\alpha} = \mathbf{h} \mathbf{B}^{-1}. \quad (18)$$

Let \mathbf{w}_i and \mathbf{W} be the weight vector and matrix that are the nonlinear counterpart of \mathbf{b}_i and \mathbf{B} , respectively. Substituting the WM smoother $\langle \mathbf{w}_i \rangle$ for the linear subfilter $y_i(n)$ in (15a), we obtain the LCWM filter defined by

$$y_{\text{LCWM}}(n) = \sum_{i=1}^K \alpha_i \langle \mathbf{w}_i \rangle. \quad (19)$$

Fig. 3 illustrates the LCWM filter structure, which is a linear combination of WM smoothers.

We can express (19) in a form similar to (17) as

$$y_{\text{LCWM}}(n) = \boldsymbol{\alpha} \langle \mathbf{W} \rangle \quad (20)$$

where

$$\langle \mathbf{W} \rangle = \left\langle \begin{bmatrix} \mathbf{w}_1 \\ \vdots \\ \mathbf{w}_K \end{bmatrix} \right\rangle = \begin{bmatrix} \langle \mathbf{w}_1 \rangle \\ \vdots \\ \langle \mathbf{w}_K \rangle \end{bmatrix}. \quad (21)$$

IV. DESIGNING LCWM FILTERS

In this section, we propose a design method for the LCWM filter that satisfies required frequency characteristics. The pro-

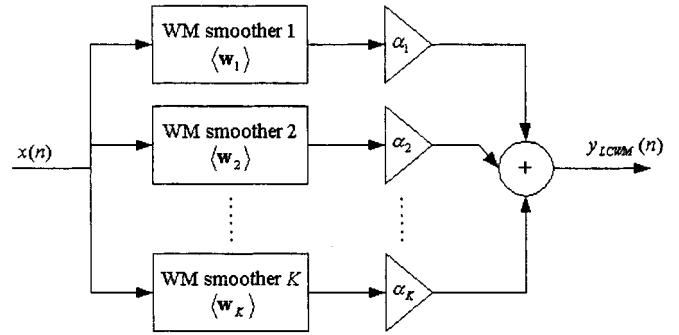


Fig. 3. LCWM filter framework.

posed method has two steps: First, a prototype FIR filter is designed. From this prototype, an LCWM filter is obtained by using a transformation that will be introduced in the next subsection.

A. Transformation From the FIR Filter to the Corresponding LCWM Filter

Before we show the main results, we provide a brief review of the basis concepts in the context of linear algebra.

A real N -dimensional vector space \mathbb{R}^N is spanned by N linearly independent vectors $\mathbf{b}_1, \dots, \mathbf{b}_N$ (with N components each). These N linearly independent sets in \mathbb{R}^N are called a *basis* for \mathbb{R}^N . That is, if a basis for \mathbb{R}^N is given, any vector \mathbf{h} with N components can be formed as a linear combination of vectors in the basis.

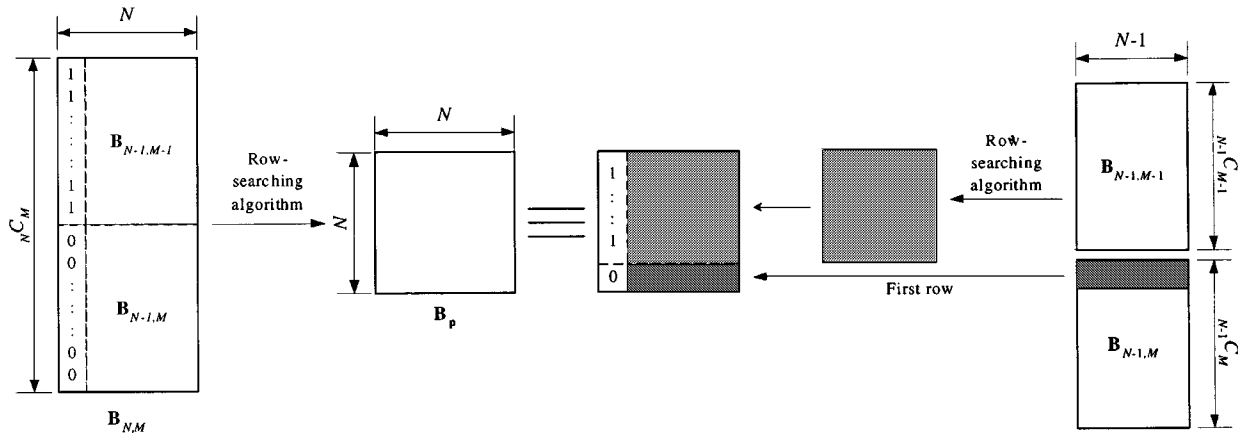
$$\mathbf{h} = \alpha_1 \mathbf{b}_1 + \dots + \alpha_N \mathbf{b}_N \quad (22a)$$

$$= \boldsymbol{\alpha} \mathbf{B}. \quad (22b)$$

Consider an FIR filter with the coefficient vector \mathbf{h} . Then, from (22a), the filter \mathbf{h} can be formed as a linear combination of subfilter coefficient vectors $\mathbf{b}_1, \dots, \mathbf{b}_N$, namely, the basis for \mathbf{h} . Note that (22b) is identical to (18). The question, then, is how we can determine the basis matrix \mathbf{B} . Before we introduce the method to determine the basis, we briefly review the combination theory.

An M -combination of an N -set is a subset with M elements chosen from the set with N elements. For example, the 2-combinations of set $\{e_1, e_2, e_3, e_4\}$ are $\{e_1, e_2\}$, $\{e_1, e_3\}$, $\{e_1, e_4\}$, $\{e_2, e_3\}$, $\{e_2, e_4\}$, and $\{e_3, e_4\}$. For simplicity in the manipulation, each combination is denoted in vector form, such as $[1 \ 1 \ 0 \ 0]$ for $\{e_1, e_2\}$. The number of M -combinations of an N -set is the binomial coefficient ${}_N C_M = N!/(M!(N-M)!) = L$. Let $\mathbf{B}_{N,M}$ denote an $L \times N$ combination matrix consisting of the combination vectors. The matrix $\mathbf{B}_{N,M}$ can be easily obtained using the classic recursive relation for binomial coefficients ${}_N C_M = {}_{N-1} C_M + {}_{N-1} C_{M-1}$ as follows:

$$\mathbf{B}_{N,M} = \left[\begin{array}{c|c} 1 & \mathbf{B}_{N-1,M-1} \\ \vdots & \\ 1 & \\ \hline 0 & \mathbf{B}_{N-1,M} \\ \vdots & \\ 0 & \end{array} \right] \quad (23)$$

Fig. 4. Recursive properties of \mathbf{B}_p and $\mathbf{B}_{N,M}$.

where

$$\mathbf{B}_{t,t} = \underbrace{[1 \ 1 \ \cdots \ 1]}_{t \text{ times}}$$

and $\mathbf{B}_{m,1}$ is the $m \times m$ identity matrix. For example

$$\mathbf{B}_{5,3} = \begin{bmatrix} 1 & 1 & 1 & 0 & 0 \\ 1 & 1 & 0 & 1 & 0 \\ 1 & 1 & 0 & 0 & 1 \\ 1 & 0 & 1 & 1 & 0 \\ 1 & 0 & 1 & 0 & 1 \\ 1 & 0 & 0 & 1 & 1 \\ 0 & 1 & 1 & 1 & 0 \\ 0 & 1 & 1 & 0 & 1 \\ 0 & 1 & 0 & 1 & 1 \\ 0 & 0 & 1 & 1 & 1 \end{bmatrix}. \quad (24)$$

With the *row-searching algorithm* [17], one can find a unique $N \times N$ matrix \mathbf{B}_p by selecting linearly independent rows of $\mathbf{B}_{N,M}$. For example, applying the row-searching algorithm to the matrix in (24) gives

$$\mathbf{B}_p = \begin{bmatrix} 1 & 1 & 1 & 0 & 0 \\ 1 & 1 & 0 & 1 & 0 \\ 1 & 1 & 0 & 0 & 1 \\ 1 & 0 & 1 & 1 & 0 \\ 0 & 1 & 1 & 1 & 0 \end{bmatrix} \quad (25)$$

whose rank, which is denoted by $\rho(\mathbf{B}_p)$, is equal to 5.

The matrix \mathbf{B}_p can be also obtained by using the recursive property of $\mathbf{B}_{N,M}$, as shown in Fig. 4. Since $\mathbf{B}_{N,M}$ consists of N linearly independent vectors, the submatrix $\mathbf{B}_{N-1,M-1}$ has $(N-1)$ linearly independent rows. Appending 1s to the beginning of each $(N-1)$ linearly independent row of $\mathbf{B}_{N-1,M-1}$ provides the first $(N-1)$ rows of \mathbf{B}_p . The last row of \mathbf{B}_p is obtained by appending 0 to the beginning of the first row of $\mathbf{B}_{N-1,M}$.

For a given \mathbf{h} , the basis matrix \mathbf{B} defined in (22b) is obtained by replacing the 1s of each row in \mathbf{B}_p with M nonzero SSPs of the nonlinear subfilters constituting the LCWM filter. Theoretically, the weights of the subfilters can be arbitrary only if the corresponding SSPs are nonzeros. In this paper, we restrict our attention to a simple case where the subfilters are the standard

median smoothers, that is, the SSP and \mathbf{B}_p are $1/M$ and \mathbf{W} , respectively.

Next, we summarize the design procedure for the LCWM filter.

Design Procedure for the LCWM Filter:

- 1) Design an N -tap prototype FIR filter \mathbf{h} using frequency specifications.
- 2) Choose a weight vector \mathbf{w} of the M -tap SM subfilter (smoother) ($M < N$).
- 3) Using the row-searching algorithm, find $\mathbf{B}_{N,M}$, and convert it into $\mathbf{B}_p (= \mathbf{W})$.
- 4) Using SSPs and $1/M$ s, transform \mathbf{B}_p into \mathbf{B} .
- 5) Using (18), obtain α .

The following example shows that LCWM filter can have similar HP characteristics.

Example 1: Consider a six-tap FIR filter with coefficient vector $\mathbf{h} = [-0.3327 \ 0.8069 \ -0.4599 \ -0.1350 \ 0.0854 \ 0.0352]$, which is the decomposition HP filter of Daubechies wavelet. Design LCWM filter that has 3-tap subfilters.

The corresponding SSP's of the weights are $[1/3 \ 1/3 \ 1/3]$. Using the above design procedure, we obtain the basis matrices of LCWM \mathbf{B} as follows:

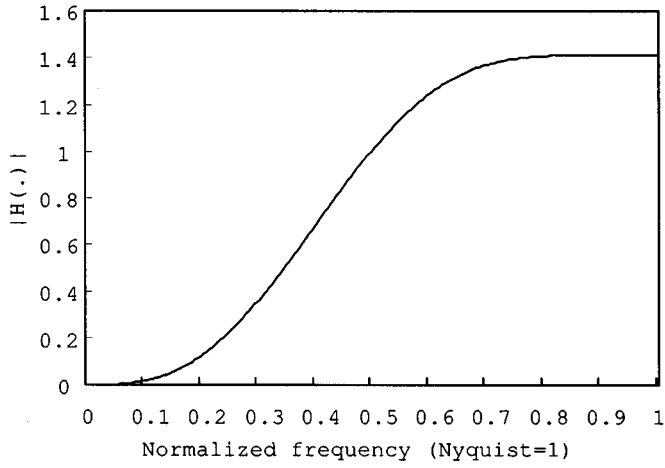
$$\mathbf{B} = \begin{bmatrix} \frac{1}{3} & \frac{1}{3} & \frac{1}{3} & 0 & 0 & 0 \\ \frac{1}{3} & \frac{1}{3} & 0 & \frac{1}{3} & 0 & 0 \\ \frac{1}{3} & \frac{1}{3} & 0 & 0 & \frac{1}{3} & 0 \\ \frac{1}{3} & \frac{1}{3} & 0 & 0 & 0 & \frac{1}{3} \\ \frac{1}{3} & 0 & \frac{1}{3} & \frac{1}{3} & 0 & 0 \\ 0 & \frac{1}{3} & \frac{1}{3} & \frac{1}{3} & 0 & 0 \end{bmatrix}. \quad (26)$$

The weighting factor vectors for each case are determined by $\alpha = \mathbf{h}\mathbf{B}^{-1} = [0.0430 \ 1.0176 \ 0.2563 \ 0.1057 \ -2.4207 \ 0.9980]$. Therefore, LCWM is given by

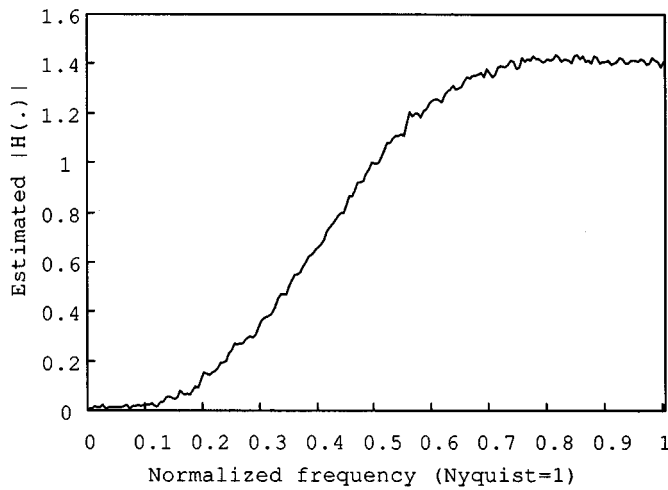
$$y_{\text{LCWM}}(n) = \alpha \langle \mathbf{W} \rangle$$

$$= \begin{bmatrix} 0.0430 \\ 1.0176 \\ 0.2563 \\ 0.1057 \\ -2.4207 \\ 0.9980 \end{bmatrix}^T \left\langle \begin{bmatrix} 1 & 1 & 1 & 0 & 0 & 0 \\ 1 & 1 & 0 & 1 & 0 & 0 \\ 1 & 1 & 0 & 0 & 1 & 0 \\ 1 & 1 & 0 & 0 & 0 & 1 \\ 1 & 0 & 1 & 1 & 0 & 0 \\ 0 & 1 & 1 & 1 & 0 & 0 \end{bmatrix} \right\rangle.$$

■



(a)



(b)

Fig. 5. (Estimated) HP frequency response. (a) Frequency response of the HP filter of Daubechies wavelet. (b) Estimated frequency response of the LCWM filter with $\mathbf{w} = [1 \ 1 \ 1]$.

Fig. 5(b) shows the estimated frequency response of the above LCWM filter. For comparison, the frequency response of the HP filter with Daubechies wavelet is also presented. It is seen that the LCWM filter exhibits similar HP characteristics as the linear filter.

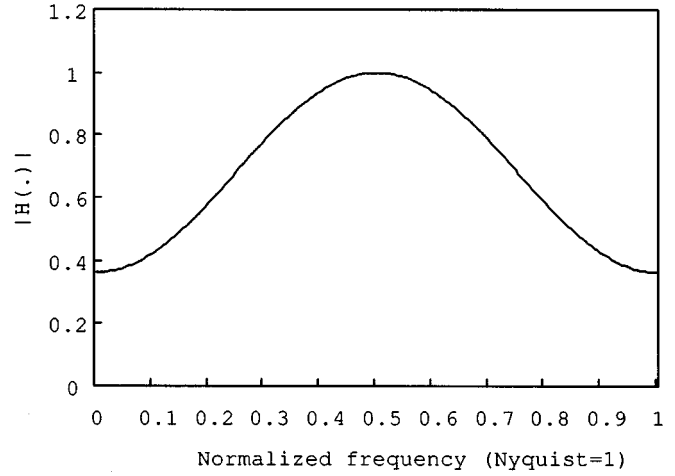
B. Symmetric LCWM Filter

Under the assumption that the FIR filter is of linear phase, the number of subfilters of the LCWM filter can be reduced. An odd-length linear-phase FIR filter with $\mathbf{h} = [h(0) \ h(1) \ \dots \ h(2N)]$ is defined as a filter that has a symmetric impulse response

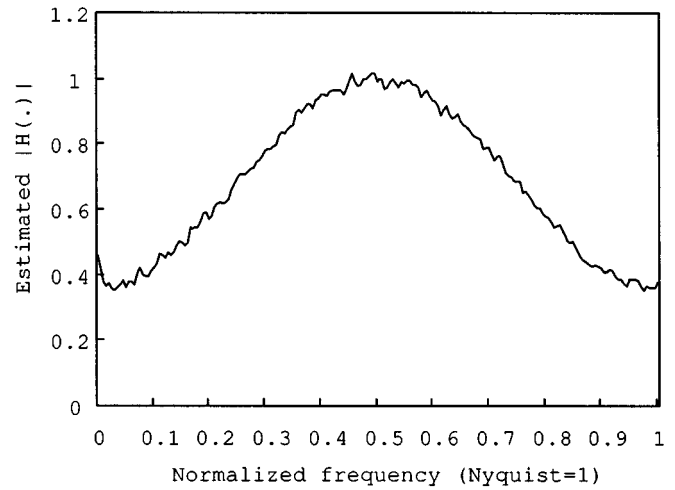
$$h(n) = h(2N - n), \quad 0 \leq n < 2N + 1 \quad (27)$$

where N is an integer. Thus, the linear-phase FIR filter can be formulated as

$$y(n) = h(N)x(n - N) + \sum_{k=0}^{N-1} h(k)(x(n - k) + x(n + k - 2N)). \quad (28)$$



(a)



(b)

Fig. 6. (Estimated) BP frequency response. (a) Frequency response of the prototype BP FIR filter. (b) Estimated frequency response of the LCWM filter designed with $\mathbf{w} = [1 \ 1 \ 1 \ 1 \ 1]$.

Note that the $(2N + 1)$ -tap linear-phase FIR filter has $(N + 1)$ independent coefficients.

Let the vector consisting of these $(N + 1)$ independent coefficients be denoted by $\mathbf{h}' = [h_1 \ h_2 \ \dots \ h_{N+1}]$ with $h_i = h(N + i - 1)$. The reduced number $(N + 1)$ of coefficients leads to a reduced $(N + 1) \times (N + 1)$ basis matrix. If we form a $(2N + 1)$ -tap linear-phase FIR filter as a linear combination of linear-phase FIR subfilters with length $(2M + 1)$, we can obtain a matrix denoted by \mathbf{B}'_p , which consists of $(N + 1)$ linear independent rows of $\mathbf{B}_{N+1, M+1}$. For example, for $N + 1 = 5$ and $M + 1 = 3$, \mathbf{B}'_p is equivalent to (25). From the relationship between \mathbf{h} and \mathbf{h}' , the matrix \mathbf{B}_p for the original $(2N + 1)$ -tap linear-phase FIR filter can be obtained by left-unfolding \mathbf{B}'_p with respect to its first column as follows:

$$\mathbf{B}_p = \left[\begin{array}{cccc|c|cccc} 0 & 0 & 1 & 1 & 1 & 1 & 1 & 0 & 0 \\ 0 & 1 & 0 & 1 & 1 & 1 & 0 & 1 & 0 \\ 1 & 0 & 0 & 1 & 1 & 1 & 0 & 0 & 1 \\ 0 & 1 & 1 & 0 & 1 & 0 & 1 & 1 & 0 \\ 0 & 1 & 1 & 1 & 0 & 1 & 1 & 1 & 0 \end{array} \right] \quad (29)$$

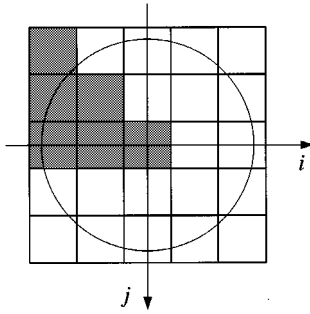


Fig. 7. Two-dimensional circularly symmetric FIR filter with the eight-fold symmetry.

where each row represents the subwindow pattern of each $(2M + 1 = 5)$ -tap linear-phase subfilter, except that the last one represents a $(2M + 2 = 6)$ -tap subfilter because the even number of ones in the last row and the “0” in the middle of the last row are rendered by the characteristic of \mathbf{B}_p (here, \mathbf{B}'_p) as shown in Fig. 4.

As in the previous subsection, an $(N + 1) \times (N + 1)$ basis matrix \mathbf{B}' for \mathbf{h}' can be obtained by placing appropriate SSPs at the nonzero positions of \mathbf{B}'_p . Then, the weighting factor vector α is determined by

$$\alpha = \mathbf{h}'(\mathbf{B}')^{-1}. \quad (30)$$

Example 2: Consider a filter coefficient vector $\mathbf{h} = [0 \ -0.1597 \ 0 \ 0.6806 \ 0 \ -0.1597 \ 0]$ that is a 7-tap $(2N + 1 = 7)$ BP filter with cut-off frequencies $[0.3 \ 0.7]$ designed by MATLAB. Using the symmetric length-five $(2M + 1 = 5)$ median filter, design the corresponding LCWM filter.

For $N + 1 = 4$ and $M + 1 = 3$, we have

$$\mathbf{B}'_p = \mathbf{B}_{4,3} = \begin{bmatrix} 1 & 1 & 1 & 0 \\ 1 & 1 & 0 & 1 \\ 1 & 0 & 1 & 1 \\ 0 & 1 & 1 & 1 \end{bmatrix}. \quad (31)$$

Then, \mathbf{B}_p is given by

$$\mathbf{B}_p = \begin{bmatrix} 0 & 1 & 1 & 1 & 1 & 1 & 0 \\ 1 & 0 & 1 & 1 & 1 & 0 & 1 \\ 1 & 1 & 0 & 1 & 0 & 1 & 1 \\ 1 & 1 & 1 & 0 & 1 & 1 & 1 \end{bmatrix}. \quad (32)$$

Since the first three rows and the last row represent 5-tap and 6-tap median filters, respectively, replacing 1s of the first three rows in (31) with $[1/5 \ 1/5 \ 1/5]$ and 1s of the last row with $[1/6 \ 1/6 \ 1/6]$ yields

$$\mathbf{B}' = \begin{bmatrix} \frac{1}{5} & \frac{1}{5} & \frac{1}{5} & 0 \\ \frac{1}{5} & \frac{1}{5} & 0 & \frac{1}{5} \\ \frac{1}{5} & 0 & \frac{1}{5} & \frac{1}{5} \\ 0 & \frac{1}{6} & \frac{1}{6} & \frac{1}{6} \end{bmatrix}. \quad (33)$$

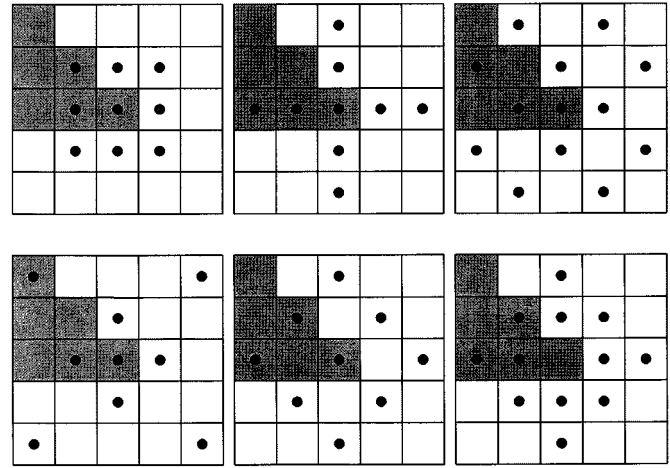


Fig. 8. 5×5 subwindow patterns, where the dotted pixels indicates nonzero element positions.

Using (30) with $\mathbf{h}' = [0.6806 \ 0 \ -0.1597 \ 0]$, we obtain $\alpha = [0.8682 \ 1.6667 \ 0.8682 \ -3.0418]$. Subsequently, the LCWM filter is given by

$$y_{\text{LCWM}}(n) = \alpha \langle \mathbf{W} \rangle = \begin{bmatrix} 0.8682 \\ 1.6667 \\ 0.8682 \\ -3.0418 \end{bmatrix}^T \left\langle \begin{bmatrix} 0 & 1 & 1 & 1 & 1 & 1 & 0 \\ 1 & 0 & 1 & 1 & 1 & 0 & 1 \\ 1 & 1 & 0 & 1 & 0 & 1 & 1 \\ 1 & 1 & 1 & 0 & 1 & 1 & 1 \end{bmatrix} \right\rangle. \quad (34)$$

The estimated frequency response of the resultant LCWM filter is shown in Fig. 6.

C. 2-D Symmetric LCWM Filter

In image processing, to prevent the image distortion, a 2-D circularly symmetric filter having zero-phase is usually used [18]. Its impulse response is circularly symmetric with respect to the center of the window (the origin). The design scheme for the 1-D symmetric LCWM filter introduced in the previous subsection can be easily extended to the design method for the 2-D circularly symmetric LCWM filter.

As mentioned before, imposing symmetry constraints reduces the number of filter coefficients. Consider a circularly symmetric filter with an eight-fold symmetry given by

$$h(i, j) = h(-i, j) = h(i, -j) = h(j, i). \quad (35)$$

For the circularly symmetric filter with $(2N + 1) \times (2N + 1)$ square shape, specifying $((N + 1)(N + 2))/2 = N_1$ independent points in the shaded region in Fig. 7 completely specifies $h(i, j)$ for all (i, j) .

A 1-D coefficient

$$\mathbf{h}' = \overbrace{[h(0, 0) \ h(-1, 0) \ \cdots \ h(-N, -N)]}^{N_1 \text{ elements}}$$

is obtained by rearranging the independent points according to their Euclidean distance from the origin. This reconfiguration converts the 2-D design problem into an 1-D design problem.

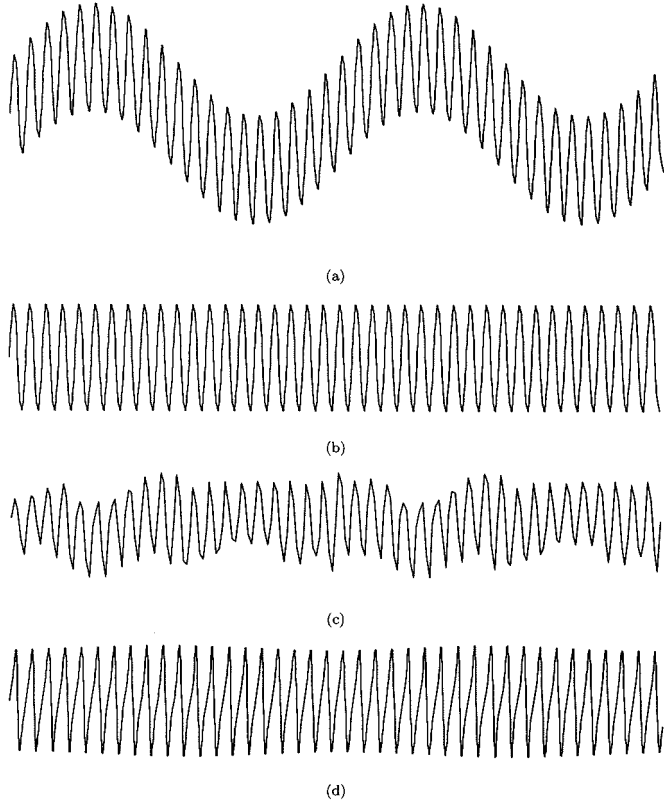


Fig. 9. (a) Two-tone input signal. (b) FIR HP filtering. (c) Optimal GWM HP filtering. (d) LCWM HP filtering.

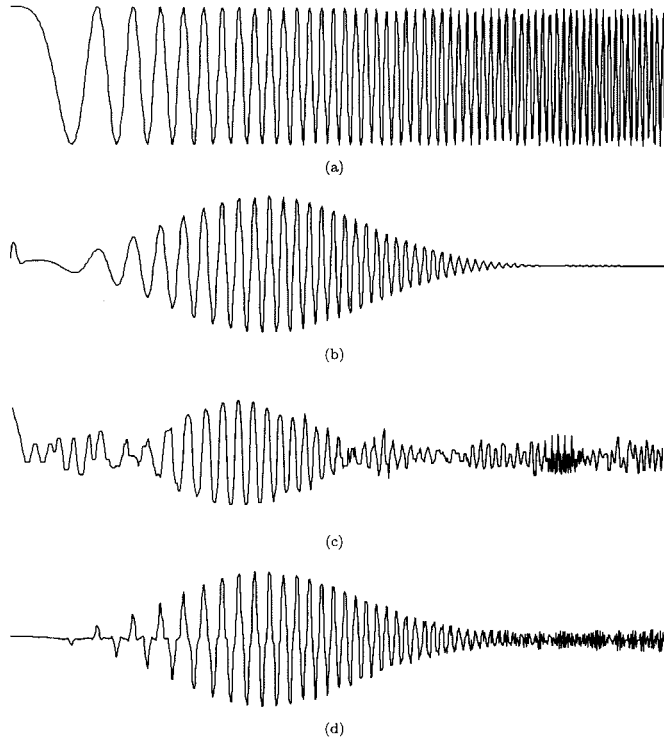


Fig. 10. Results of BP filtering of the chirp signal. (a) Chirp input signal. (b) FIR BP filtering. (c) Optimal GWM BP filtering. (d) LCWM BP filtering.

Consider a 5×5 ($N_1 = 6$) 2-D circularly symmetric filter that is formed as the linear combination of circularly symmetric sub-

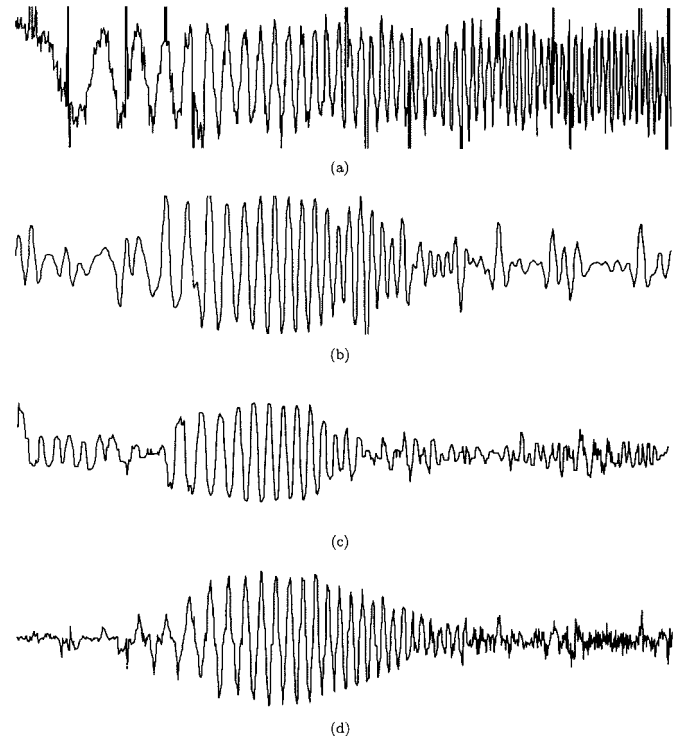


Fig. 11. Results of BP filtering of the noisy chirp signal. (a) Chirp input signal corrupted by impulses ($p = 0.05$) and Gaussian noise ($\sigma^2 = 200$). (b) FIR BP filtering. (c) Optimal GWM BP filtering. (d) LCWM BP filtering.

filters with $M_1 (= 3)$ independent points. Then, from $\mathbf{B}_{N_1, M_1} = \mathbf{B}_{6, 3}$, we obtain

$$\mathbf{B}'_{\mathbf{p}} = \begin{bmatrix} 1 & 1 & 1 & 0 & 0 & 0 \\ 1 & 1 & 0 & 1 & 0 & 0 \\ 1 & 1 & 0 & 0 & 1 & 0 \\ 1 & 1 & 0 & 0 & 0 & 1 \\ 1 & 0 & 1 & 1 & 0 & 0 \\ 0 & 1 & 1 & 1 & 0 & 0 \end{bmatrix}. \quad (36)$$

Note that each row of $\mathbf{B}'_{\mathbf{p}}$ provides the position information of zero and nonzero elements for the corresponding 2-D subwindows. For example, the first row of $\mathbf{B}'_{\mathbf{p}}$ in (36) implies that the first 2-D subfilter has three independent nonzero coefficients at positions corresponding to $h_1 = h(0, 0)$, $h_2 = h(-1, 0)$, and $h_3 = h(-1, -1)$. Using the eight-fold symmetry defined in (35), we obtain six subwindow patterns from rows of $\mathbf{B}'_{\mathbf{p}}$ in (36) (see Fig. 8). Note that each subwindow pattern has a different number of nonzero coefficients.

Example 3: Consider a 5×5 filter coefficient matrix ($N = 2$, $N_1 = 6$) given by

$$\begin{bmatrix} 0.0006 & 0.0025 & 0.0038 & 0.0025 & 0.0006 \\ 0.0025 & 0.0551 & 0.1051 & 0.0551 & 0.0025 \\ 0.0038 & 0.1051 & 0.3213 & 0.1051 & 0.0038 \\ 0.0025 & 0.0551 & 0.1051 & 0.0551 & 0.0025 \\ 0.0006 & 0.0025 & 0.0038 & 0.0025 & 0.0006 \end{bmatrix}. \quad (37)$$

The filter with the coefficient matrix in (37) is an LP filter with cut-off frequency 0.4 designed by MATLAB. Design a 2-D circularly symmetric LCWM filter consisting of circularly symmetric median subfilters with three independent weights ($M_1 = 3$).

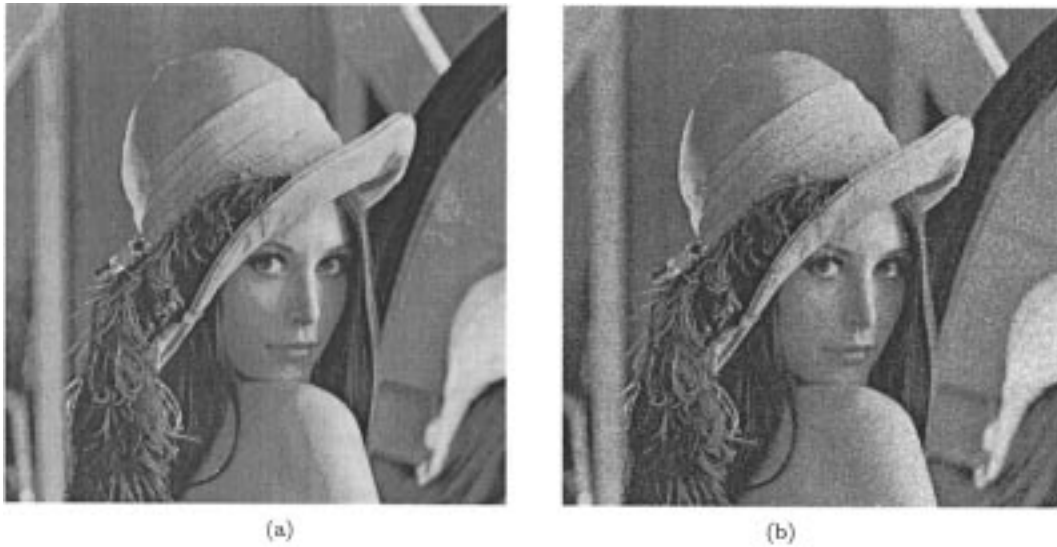


Fig. 12. (a) Original image. (b) Noisy image (Gaussian noise $\sigma^2 = 200$).

Since $N_1 = 6$ and $M_1 = 3$, \mathbf{B}'_p is identical to the matrix in (36). Arranging filter coefficients of (37) according to their Euclidean distance from the origin gives

$$\mathbf{h}' = [0.3213 \ 0.1051 \ 0.0551 \ 0.0038 \ 0.0025 \ 0.0006]$$

and replacing 1s of \mathbf{B}'_p by the corresponding SSPs, the basis matrix \mathbf{B}' for \mathbf{h}' is obtained as

$$\mathbf{B}' = \begin{bmatrix} \frac{1}{9} & \frac{1}{9} & \frac{1}{9} & 0 & 0 & 0 \\ \frac{1}{9} & \frac{1}{9} & 0 & \frac{1}{9} & 0 & 0 \\ \frac{1}{13} & \frac{1}{13} & 0 & 0 & \frac{1}{13} & 0 \\ \frac{1}{9} & \frac{1}{9} & 0 & 0 & 0 & \frac{1}{9} \\ \frac{1}{9} & 0 & \frac{1}{9} & \frac{1}{9} & 0 & 0 \\ 0 & \frac{1}{12} & \frac{1}{12} & \frac{1}{12} & 0 & 0 \end{bmatrix}. \quad (38)$$

From (30) and (38), $\alpha = [1.4031 \ 0.9414 \ 0.0325 \ 0.0054 \ 0.5193 \ -1.9020]$.

V. EXPERIMENTAL RESULTS

The frequency response characteristics of the 1-D and 2-D LCWM filters are examined and compared with those of the linear FIR and some existing nonlinear filters.

A. 1-D LCWM Filters

The HP filtering performance of the filters is tested using a two-tone signal containing two sinusoidal signals with frequencies 0.02 and 0.4 shown as Fig. 9(a) (normalized Nyquist frequency equal to 1). Fig. 9(b) shows the signal filtered by a 25-tap linear FIR filter with normalized cut-off frequency 0.35. It is seen that the FIR filter has completely removed all low-frequency components while preserving a high-frequency tone. The two-tone signal is processed by a 25-tap GWM filter optimized by the fast adaptive LMA algorithm [7]. Fig. 9(c) shows that the optimal GWM filter removes the low-frequency components while yielding some minor artifacts. In Fig. 9(d), the

TABLE I
NMSE's ASSOCIATED WITH NOISE

Filter Type (5 × 5)	NMSE			
	$\sigma^2=100$	$\sigma^2=200$	$p=0.02$ $\sigma^2=200$	$p=0.05$ $\sigma^2=200$
median	0.587	0.329	0.118	0.063
FIR	0.443	0.269	0.168	0.144
GWM	0.358	0.280	0.103	0.058
LCWM	0.340	0.254	0.095	0.055

25-tap LCWM filter consisting of symmetric median subfilters with $\mathbf{B}_{13,2}$ performs like the FIR HP filter.

In order to test BP filtering responses, a chirp signal spanning instantaneous normalized frequency ranging from 0 to 0.5 Hz is utilized. Fig. 10(b) shows the chirp signal filtered by a 31-tap FIR BP filter with normalized passband frequencies $0.1 \leq \omega \leq 0.2$. A desired signal generated by an 121-tap FIR BP filter with the same frequency specification $0.1 \leq \omega \leq 0.2$ was utilized to optimize a 31-tap GWM BP filter. Fig. 10(c) depicts the output of the 31-tap GWM BP filter. Fig. 10(d) shows the chirp signal filtered by an LCWM filter with $\mathbf{B}_{16,2}$. The BP frequency response of the GWM and LCWM filters are clearly seen.

Fig. 11 shows the performance of the filters on chirp signal degraded by impulses of probability 0.03 and zero mean i.i.d. Gaussian noise of variance 0.04. The aforementioned filters are applied to the noisy chirp signal. In Fig. 11(b)–(d), the FIR BP filter is affected by noise, whereas the GWM and LCWM BP filters show a considerable improvement.

B. 2-D LCWM Filters

For 2-D simulation, we used images consisting of 512×512 pixels with eight bits of resolution. In order to quantitatively compare the performance of the filters we have discussed, the

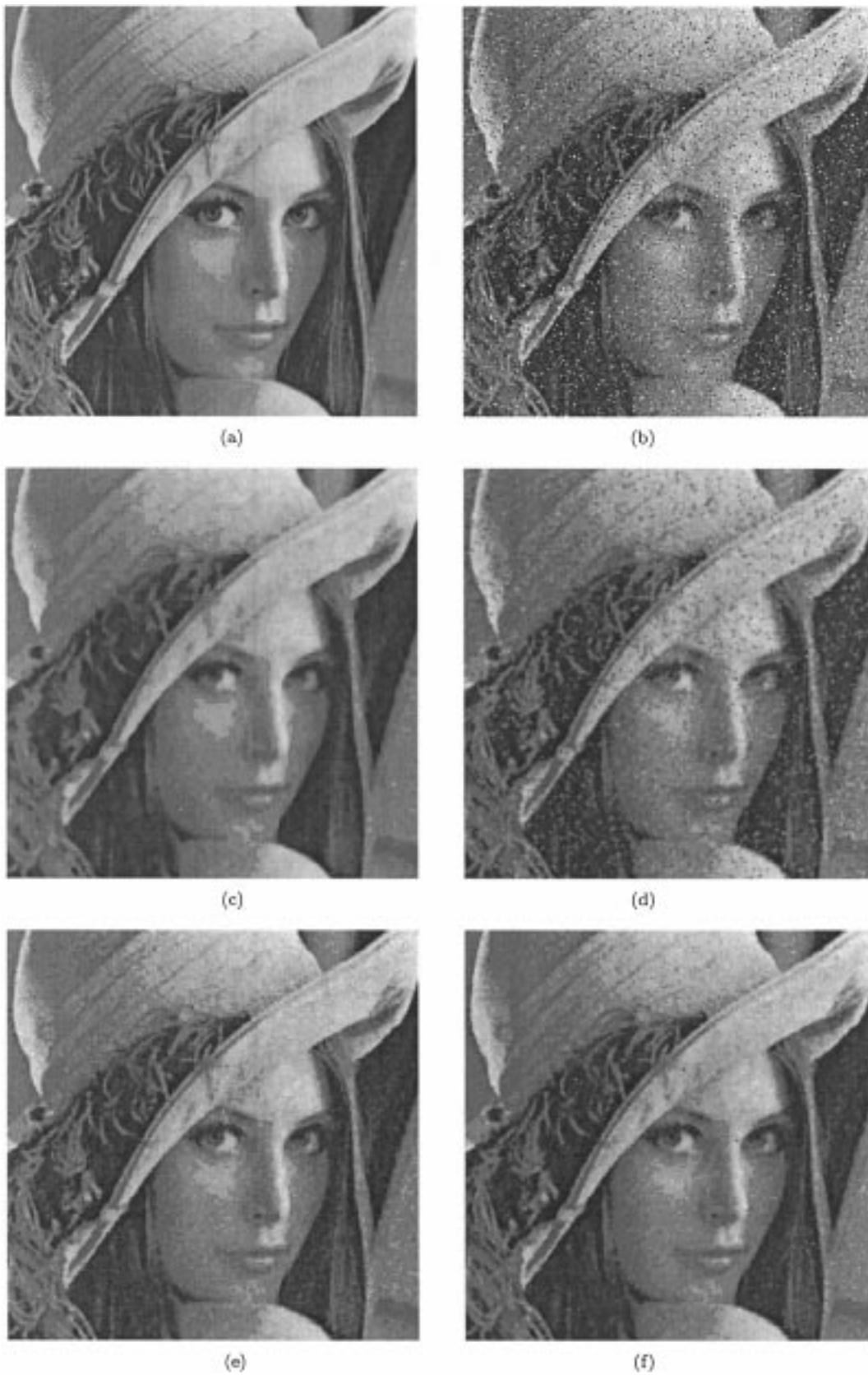


Fig. 13. LP filtering. (a) Original image. (b) Noisy image. (c) Median filtering. (d) FIR filtering. (e) GWM filtering. (f) LCWM filtering.

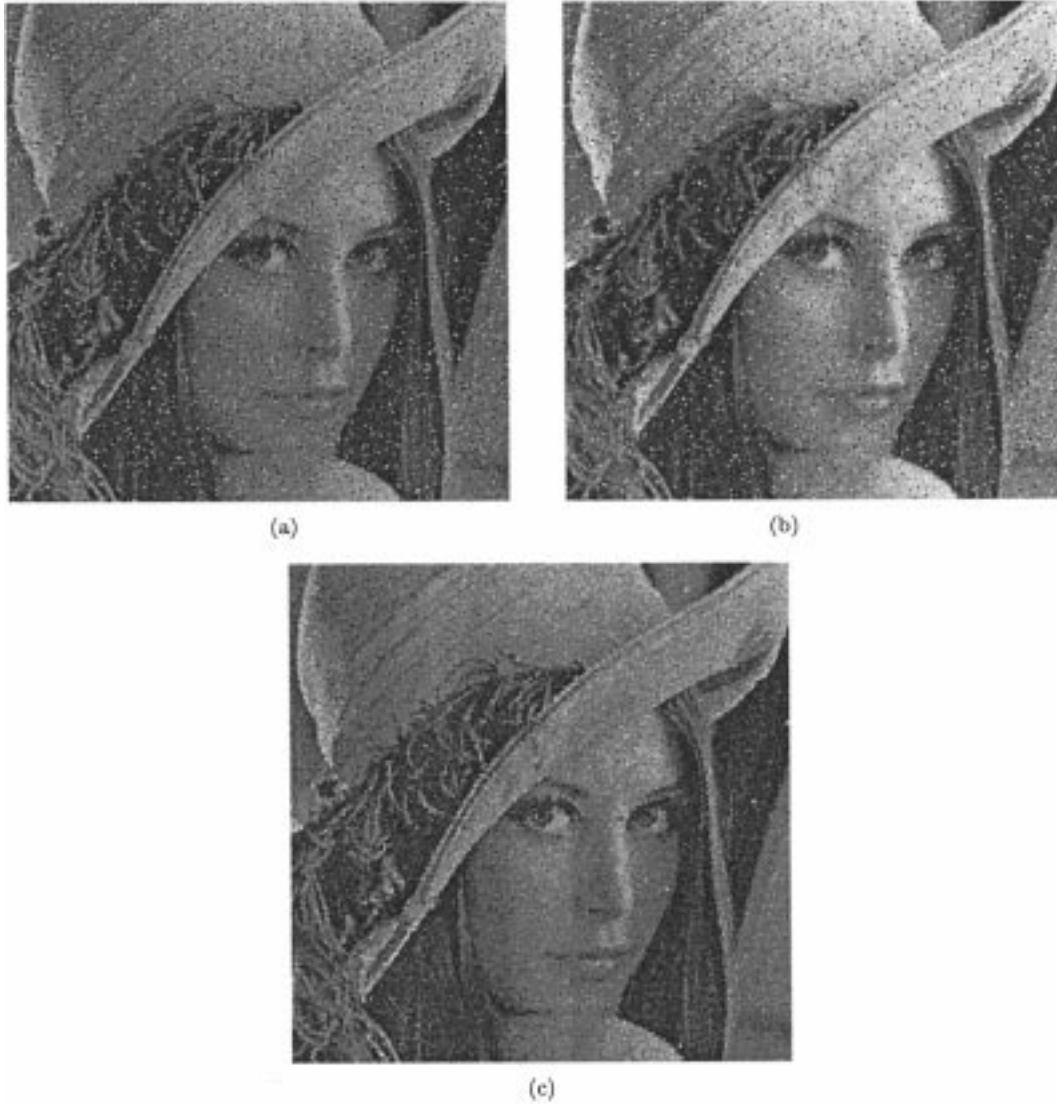


Fig. 14. BP filtering. (a) FIR filtering. (b) GWM filtering. (c) LCWM filtering.

normalized mean square error (NMSE) between the original and filtered images is evaluated. The NMSE is given by

$$\text{NMSE} = \frac{\sum_{i=0}^{L-1} \sum_{j=0}^{L-1} [Y(i, j) - S(i, j)]^2}{\sum_{i=0}^{L-1} \sum_{j=0}^{L-1} [X(i, j) - S(i, j)]^2} \quad (39)$$

where $S(i, j)$, $X(i, j)$, and $Y(i, j)$ are the original, noisy input, and filtered images, respectively, and $L = 512$. In addition, we present original and filtered images to quantify the error in human visual error criteria.

The performance of the filters discussed so far is evaluated by applying them to noisy images degraded by additive white and/or impulsive noise and then by comparing their respective results. The original noise-free image is shown in Fig. 12(a). Two noisy images were generated by adding zero mean i.i.d. Gaussian noise of variance 100 and 200 to the original image, and two Gaussian plus impulsive noisy images were obtained

by adding impulsive noise of probability 0.02 and 0.05 to the Gaussian noisy image of variance 200. Then, these four noisy images were passed through various 2-D filters with 5×5 square window. Fig. 12(b) shows the noisy image with the noise variance 200. In the following, we first compare the NMSEs of the LP filters and then visually compare some of the filtered images.

Table I summarizes the NMSEs of median, FIR, GWM, and LCWM filters. The filters except the median filter were designed based on the LP FIR filter with cut-off frequency 0.001. In each case, the LCWM filter yields the smallest NMSE.

The LP filters with 5×5 window are applied to the noisy image contaminated by zero mean i.i.d. Gaussian noise of variance 200 and impulses of probability 0.05. The GWM and LCWM LP filters are designed using the coefficients of the FIR LP filter with a normalized cut-off frequency 0.1. Fig. 13(c)–(f) shows that the median filter causes the blur, and that the FIR filter performs the worst, whereas both the LCWM and GWM filters produce satisfactory results.

The noisy image in Fig. 13(b) is filtered by the FIR, GWM, and LCWM BP filters with passband $0.3 \leq \omega \leq 0.7$.

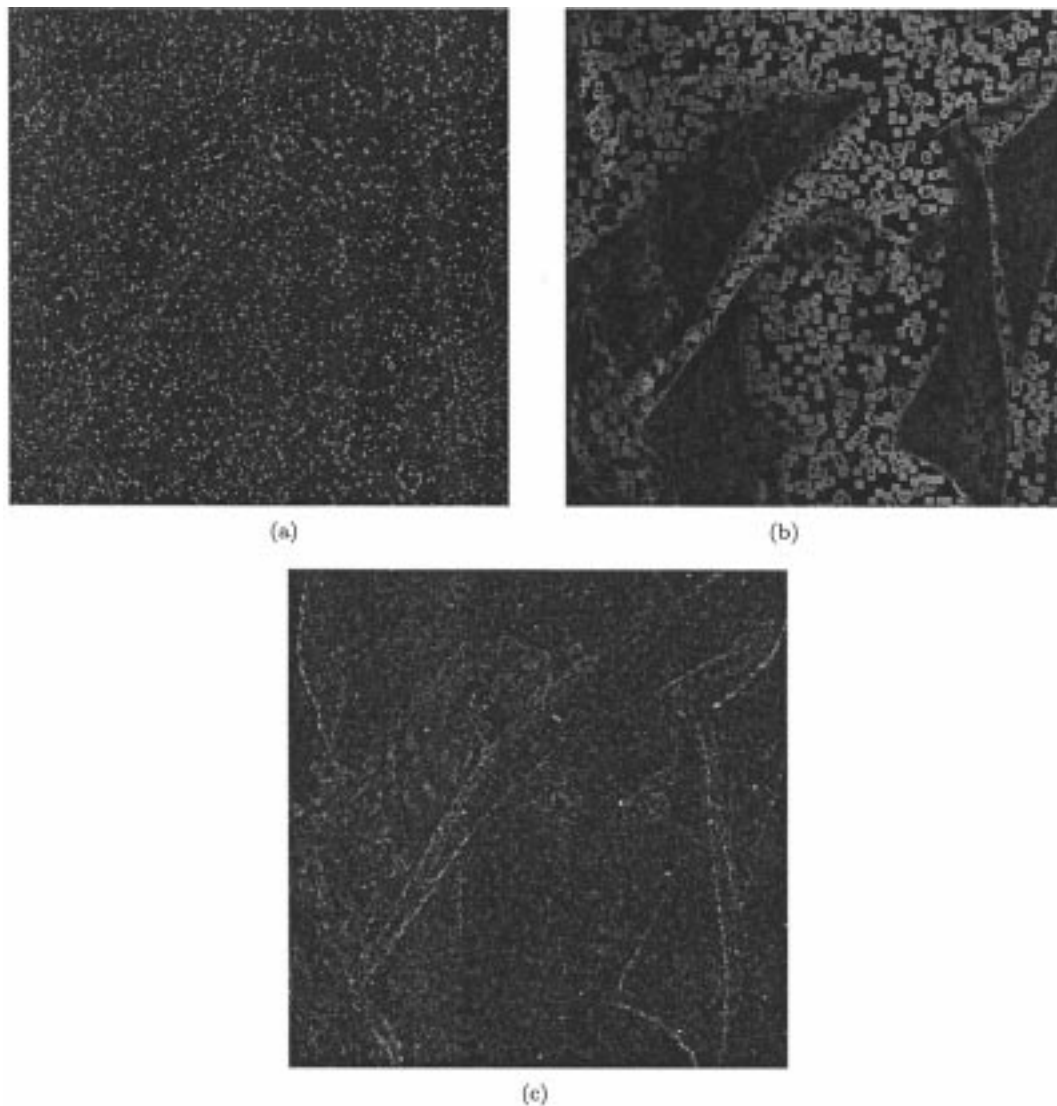


Fig. 15. HP filtering. (a) FIR filtering. (b) GWM filtering. (c) LCWM filtering.

Fig. 14(a)–(c) shows that the FIR and GWM filters do not suppress impulsive noise. Since the absolute value of the center coefficient among the FIR filter coefficients is almost as large as the absolute sum of the other coefficients, the GWM filter fails to remove the impulses. The LCWM BP filter removes both impulsive noise and Gaussian noise significantly.

The noisy image in Fig. 13(b) is processed by the FIR, GWM, and LCWM HP filters with cut-off frequency 0.7. For the purpose of display, the absolute values of the HP filtered image are taken so that edges of negative values are shown. Fig. 15(a)–(c) shows that the LCWM filter significantly attenuates the low-frequency components of images while removing impulsive noise.

VI. CONCLUSIONS

The observation on structure and design procedure of the linear FIR HP filter has brought us to the definition of the LCWM filter, which is represented as a linear combination of WM filters. The proposed filter can be considered as a generalization of the difference of estimates including the DoM.

We have presented the design method of the LCWM filters using the transform from the FIR filter to the LCWM filter. A simulation using the chirp signal and 2-D images confirmed our expectations and shows that the LCWM filter should be considered as a possible alternative to the LP, HP, and BP FIR filters in dealing with noise that present strong non-Gaussian nature.

REFERENCES

- [1] L. Yin, R. Yang, M. Gabbouj, and Y. Neuvo, "Weighted median filters: A tutorial," *IEEE Trans. Circuits Syst.*, vol. 43, pp. 157–191, Mar. 1996.
- [2] O. Yli-Harja, J. Astola, and Y. Neuvo, "Analysis of the properties of median and weighted median filters using threshold logic and stack filter representation," *IEEE Trans. Signal Processing*, vol. 39, pp. 395–410, Feb. 1991.
- [3] J. Nieweglowski, M. Gabbouj, and Y. Neuvo, "Weighted medians-positive Boolean functions conversion algorithms," *Signal Process.*, vol. 34, pp. 149–161, 1993.
- [4] M. Gabbouj, P. T. Yu, and E. J. Coyle, "Convergence behavior and root signal sets of stack filters," *Circuits, Syst. Signal Process.*, vol. 11, no. 1, pp. 171–194, 1992.
- [5] P. D. Wendt, E. J. Coyle, and J. N. C. Gallagher, "Stack filters," *IEEE Trans. Acoust., Speech, Signal Processing*, vol. ASSP-34, pp. 898–911, Aug. 1986.

- [6] C. L. Mallows, "Some theory of nonlinear smoothers," *Ann. Stat.*, vol. 8, pp. 695–715, 1980.
- [7] G. R. Arce, "A general weighted median filter structure admitting real-valued weights," *IEEE Trans. Signal Processing*, vol. 46, pp. 3195–3205, Dec. 1998.
- [8] J. L. Paredes and G. R. Arce, "Stack filters, stack smoothers, and mirrored threshold decomposition," *IEEE Trans. Signal Processing*, vol. 47, pp. 2757–2767, Oct. 1999.
- [9] G. R. Arce and J. L. Paredes, "Recursive weighted median filters admitting negative weights and their optimization," *IEEE Trans. Signal Processing*, vol. 48, pp. 768–779, Mar. 2000.
- [10] L. Yin and Y. Neuvo, "Fast adaptation and performance characteristics of fir-wos hybrid filters," *IEEE Trans. Signal Processing*, vol. 42, pp. 1610–1628, July 1994.
- [11] L. J. V. Vliet, I. T. Young, and G. L. Beckers, "A nonlinear Laplace operator as edge detector in noisy images," *Comput. Vis., Graph., Image Process.*, vol. 45, pp. 167–195, 1989.
- [12] J. S. Yoo, E. J. Coyle, and C. A. Bouman, "Dual stack filters and the modified difference of estimates approach to edge detection," *IEEE Trans. Image Processing*, vol. 6, pp. 1634–1645, Dec. 1997.
- [13] A. C. Bovik and J. D. C. Munson, "Edge detection using median comparisons," *Comput. Vision, Graph., Image Process.*, vol. 33, pp. 377–389, 1986.
- [14] A. C. Bovik, T. S. Huang, and J. D. C. Munson, "The effect of median filtering on edge estimation and detection," *IEEE Trans. Pattern Anal. Machine Intell.*, vol. PAMI-9, pp. 181–194, Mar. 1987.
- [15] G. J. Yang and T. S. Huang, "The effect of median filtering on edge location estimation," *Comput. Graph., Image Process.*, vol. 15, pp. 224–245, 1981.
- [16] K. S. Choi, K. H. Lee, S. J. Ko, and A. W. Morales, "Frequency selective weighted median filter," *Proc. SPIE*, vol. 3646, pp. 197–206, Jan. 1999.
- [17] C. Chen, *Linear System Theory and Design*. New York: CBS College, 1984.
- [18] J. S. Lim, *Two-Dimensional Signal and Image Processing*. Englewood Cliffs, NJ: Prentice-Hall, 1990.



Kang-Sun Choi (S'98) was born in Seoul, Korea. He received the B.S. and M.S. degrees in electronics engineering with the Department of Electronics Engineering from Korea University, Seoul, in 1997 and 1999, respectively. He is currently pursuing the Ph.D. degree in electrical engineering at Korea University.

In 1997, he joined the Research Institute for Information and Communication Technology, Korea University, as a Researcher. His research interests are in the areas of nonlinear signal and image processing and multimedia communications.



Aldo W. Morales (SM'99) was born in Tacna, Peru. He received the electronic engineering degree with distinction from the University of Tarapaca, Arica, Chile (formerly Northern University) and the M.S. and Ph.D. degrees in electrical and computer engineering from the State University of New York at Buffalo in 1978, 1986, and 1990, respectively.

Since September 1990, he has been with Penn State University, DuBois, PA, where he is now an Associate Professor of Engineering. His research interests are in mathematical morphology, digital

image processing, computer vision, high-definition television, and neural networks.

Dr. Morales received a Best Paper Award from the IEEE Asia Pacific Conference on Circuits and Systems in 1996, Penn State Engineering Society's Outstanding Teaching Award for 1999, and Educator of the Year, Penn State University-DuBois Campus, for 1998.



Sung-Jea Ko (M'88–SM'97) received the B.S. degree in electronic engineering from Korea University, Seoul, in 1980 and the M.S. degree in 1986 and the Ph.D. degree in 1988, both in electrical and computer engineering from State University of New York at Buffalo.

In 1992, he joined the Department of Electronic Engineering at Korea University, where he is currently a Professor. From 1988 to 1992, he was an Assistant Professor of electrical and computer engineering at the University of Michigan, Dearborn.

From 1981 to 1983, he was with Daewoo Telecom Corporation, where he was involved in research and development on data communication systems. He was Associate Editor for the *Journal of Communications and Networks* from 1998 to 2000. His current research interests are in the areas of digital signal and image processing and multimedia communications.

Dr. Ko received the Hae-Dong best paper award from the Institute of Electronics Engineers of Korea in 1997, a Best Paper Award from the IEEE Asia Pacific Conference on Circuits and Systems in 1996, and the LG Academic Award for Outstanding Research in Information and Communication from LG Electronics Inc. in 1999. He is presently Chair of IEEE Consumer Electronics Chapter in Korea and a Fellow of the IEE.